



ELSEVIER

Biochimica et Biophysica Acta 1382 (1998) 129–136



# $^1\text{H}$ and $^{13}\text{C}$ NMR studies of a truncated heme domain from *Chlorella vulgaris* nitrate reductase: signal assignment of the heme moiety

Xiangdong Wei <sup>a</sup>, Li-June Ming <sup>a,\*</sup>, Andrew C. Cannons <sup>b</sup>, Larry P. Solomonson <sup>c</sup>

<sup>a</sup> Department of Chemistry and Institute for Biomolecular Science, University of South Florida, Tampa, FL 33620-5250, USA

<sup>b</sup> Department of Biology and Institute for Biomolecular Science, University of South Florida, Tampa, FL 36620, USA

<sup>c</sup> Department of Biochemistry and Molecular Biology, College of Medicine and Institute for Biomolecular Science, University of South Florida, Tampa, FL 33612, USA

Received 9 July 1997; accepted 3 September 1997

## Abstract

A water soluble truncated heme domain (a tetramer of MW = 45 kDa) of the tetrameric nitrate reductase complex from the green alga *Chlorella vulgaris* has been overexpressed and purified. This truncated heme domain with four identical subunits has a high redox potential (midpoint potential  $E_{1/2} = +16\text{ mV}$ ) as compared with other heme-containing flavoproteins. We have undertaken a determination of the detailed configuration of the heme moiety in order to understand the unique electrochemical property of the heme moiety of this enzyme. We report here the study of the heme prosthetic group of the truncated heme domain by the use of 2D  $^1\text{H}$  and  $^{13}\text{C}$  NMR techniques. A complete signal assignment of the heme has been achieved. Our observations suggest that the heme configuration is similar to that of the crystal structure of the membrane-bound bovine liver cytochrome  $b_5$ . © 1998 Elsevier Science B.V.

**Keywords:** 2D NMR; Heme protein; Cytochrome  $b$ ; Nitrate reductase; (*Chlorella*)

## 1. Introduction

Nitrate assimilation and nitrogen fixation are the two major pathways in the biological nitrogen cycle which provide common nitrogen sources for the synthesis and utilization of proteins and nucleic acids in all living organisms. Since the available nitrogen in the form of  $\text{NH}_4^+$  in the biosphere is rather limited, a direct conversion from different inorganic forms of nitrogen to ammonia plays a crucial role, i.e. from  $\text{NO}_3^-$  via nitrate assimilation and from  $\text{N}_2$  by nitro-

gen fixation. Through nitrate assimilation, higher plants, algae, filamentous fungi, yeasts, and bacteria are able to produce more than  $2 \times 10^4$  megatons of organic nitrogen per year, which is 100-times more than that produced by nitrogen fixation [1–3]. Biological conversion of nitrate to ammonium is an eight-electron reduction process with the participation of two enzymes, the reduction of nitrate to nitrite by nitrate reductase, and the reduction of nitrite to ammonium by nitrite reductase [4]. Nitrate reductase (NR) is a multi-domain enzyme comprising the prosthetic groups molybdopterin, Fe-heme, and FAD (flavin adenine dinucleotide) in a 1:1:1 stoichiometry that mediates an electron transfer from NAD(P)H to nitrate. The FAD and Mo-pterin domains function as

\* Corresponding author. Fax: +1(813) 974-1733; E-mail: ming@chuma.cas.usf.edu

the binding sites for NAD(P)H and  $\text{NO}_3^-$ , respectively [5–7], while the cytochrome  $b_5$ -like heme domain facilitates the electron transfer from the FAD domain to the active-site Mo-pterin [8].

Mammalian liver cytochrome  $b_5$  is a membrane-bound protein that adds a practical difficulty in its isolation [9–11]. Recently, we have successfully cloned and expressed a cDNA encoding a water-soluble homo-tetrameric cytochrome  $b_5$ -like domain (MW = 45 kDa) of *Chlorella vulgaris* NR in *Escherichia coli* [6], and have studied its electrochemical and spectroscopic properties [5,12–17]. Potentiometric titration for this recombinant truncated heme domain [5] yields a midpoint potential of +16 mV ( $n = 1$ , pH 7), which is substantially higher than that for the intact NR (–160 mV) [13] and that for the recombinant NR-heme domain coupled to a truncated Mo-pterin domain (–28 mV) [5]. The expression of a large quantity of this NR-heme domain allows the study of its structure by means of NMR techniques in order to provide more information about the correlation between its structure and physical properties. Moreover, this soluble NR-heme domain can serve as a spectroscopic model for membrane-bound cytochrome  $b_5$ .

A low-spin ( $S = 1/2$ )  $\text{Fe}^{3+}$ -heme center is known to exhibit well resolved hyperfine-shifted (i.e., isotropically shifted)  $^1\text{H}$  NMR signals attributable to the protons on the heme and in its surroundings. The study of these signals can thus reveal the structure of the heme environment. Despite its paramagnetism (which is generally not favorable for 2D NMR studies), the low-spin  $\text{Fe}^{3+}$ -heme center in several proteins has recently been investigated by the use of various 2D NMR techniques [18–20]. Standard 2D NMR pulse sequences with appropriate adjustments of acquisition parameters can give spectra for paramagnetic molecules which provide virtually the same structural information as that obtained for diamagnetic molecules. For example, the use of coherence transfer techniques (COSY and TOCSY) allows the assignment of spin patterns, and the use of NOE techniques (NOESY) can reveal spatial arrangement of nuclei [21–23]. In this report, we present a complete assignment of the isotropically shifted  $^1\text{H}$  NMR signals of the heme moiety in the truncated NR-heme domain by the use of homonuclear  $^1\text{H}$ – $^1\text{H}$  and heteronuclear  $^1\text{H}$ – $^{13}\text{C}$  2D NMR techniques. These stud-

ies represent the first steps toward a complete structural analysis of the heme-binding pocket, which is a key element for a better understanding of the unusual redox property of the heme domain in nitrate reductase.

## 2. Materials and methods

The expression and purification of *Chlorella vulgaris* NR-heme domain followed the procedures reported previously [5,6]. All NMR experiments were performed on a Bruker AMX360 spectrometer at 360.13 MHz for  $^1\text{H}$  and 90.56 MHz for  $^{13}\text{C}$ . A 90° pulse of  $\sim 7 \mu\text{s}$  with a presaturation on the water signal was used for normal 1D  $^1\text{H}$  NMR spectra. A 5 Hz line broadening was introduced to the spectra via an exponential multiplication of the FIDs prior to Fourier transformation in order to improve their signal-to-noise ratios. In some cases, Gaussian line-broadening (10 to 30% shift and a line broadening factor of –30 to –50 Hz) was used to improve spectral resolution. Proton spin-lattice relaxation times ( $T_1$ ) were determined by the use of the inversion recovery method ( $180^\circ - \tau - 90^\circ$ ) with 16 different  $\tau$  values and a recycle time five times longer than the longest relaxation time of the signals of interest. The  $T_1$  values were obtained by a three-parameters fitting of the signal intensity versus the delay time  $\tau$ .

Magnitude-COSY [24] and phase sensitive (TPPI) NOESY [25,26] pulse sequences were used for the detection of coherence transfer and cross relaxation with a presaturation pulse on the water signal during the relaxation delay and mixing period. A typical 2D spectrum consisted of 1024(f2)  $\times$  512(f1) data points, a short repetition time of  $\sim 500$  ms to suppress the diamagnetic features, and a bandwidth of 21.6 kHz in both dimensions to cover the hyperfine-shifted signals. Since all the heme proton signals have relaxation times ( $T_1$ ) shorter than 130 ms, they are not saturated to a great extent by this 500 ms repetition time. In the COSY spectra, a 0°-shifted sine bell-squared window function was applied to both dimensions of the spectra prior to Fourier transformation and processed in magnitude mode without a spectral symmetrization; whereas a 45°-shifted sine-squared bell was used in NOESY experiments. The total

acquisition time in a 2D experiment for a  $\sim 4$  mM sample was usually around 12 h with 200 to 400 number of transients. Experiments were also performed at various temperatures in order to resolve overlapped signals.

The  $^1\text{H}\{^{13}\text{C}\}$  heteronuclear multiple quantum coherence (HMQC) [27,28] experiment in the phase sensitive (TPPI) mode was performed by using the BIRD sequence for spin-lock of  $^{13}\text{C}$ , and a proton-decoupling during acquisition using the GARP1 pulse sequence [27,28]. The delay for inversion recovery optimize to give null for protons bound to  $^{12}\text{C}$  had been set to a relatively long 500 ms in order to obtain a spectrum with less baseline distortion in the diamagnetic region. A delay of 200 ms and less did not give a spectrum comparable to the one shown here due to worse baseline distortion. The total time for the HMQC experiment on a sample ( $\sim 5$  mM heme concentration) at  $^{13}\text{C}$  natural abundance was 36 h with a total of  $3 \times 1800$  transients.

### 3. Results and discussion

A freshly purified sample of the recombinant NR-heme domain is recognized clearly from its  $^1\text{H}$  NMR spectrum to be a mixture of two species, with the major species 2–3 times as abundant as the minor species. The two species are under a slow equilibrium as revealed by NMR, where the  $^1\text{H}$  NMR signals of the minor species decrease in intensity and reach 1/8 the intensity of the major species in a few months at  $4^\circ\text{C}$  (Fig. 1). A similar result was also observed on a soluble truncated fragment of a membrane-bound cytochrome  $b_5$  [29–32] and on a recombinant hemoglobin from a marine annelid [33], where a protoporphyrin IX binding to the protein in two different orientations with respect to the  $\alpha$ – $\gamma$  axis was suggested.

This protein has been previously determined to be a tetramer of 45 kDa based on gel filtration and gel electrophoresis [5,6]. This has also been confirmed by

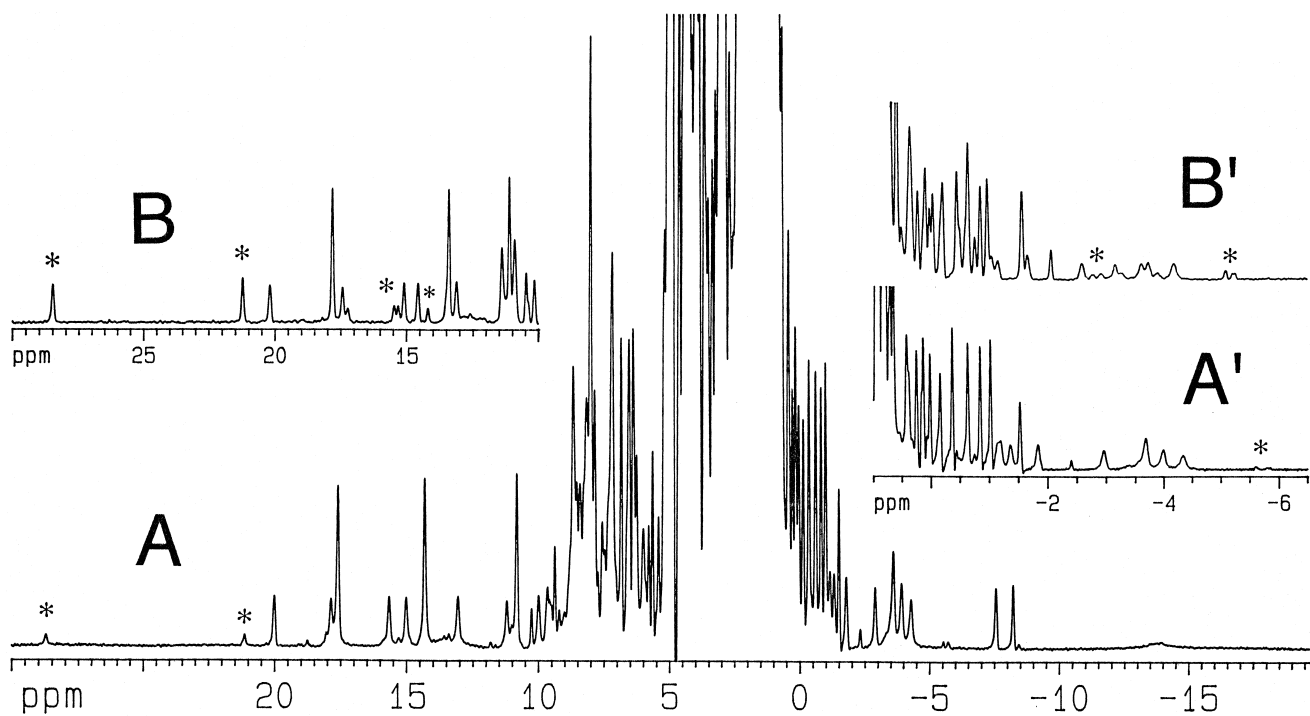


Fig. 1. Proton NMR spectrum (360.13 MHz and 298 K) of NR-heme domain stored at  $4^\circ\text{C}$  for a few months in  $\text{D}_2\text{O}$  at pH 7 (A and A'). The insets (B and B') are the regions of the  $^1\text{H}$  NMR spectrum (360.13 MHz and 300 K) which show that a freshly prepared sample of the protein in  $\text{H}_2\text{O}$  at pH 7 is a mixture of two "different proteins" with the heme bound in different orientations. The decrease of the "minor species" with time is clearly shown in the spectra. Some signals due to the "minor species" are marked with asterisks. Three heme methyl signals in the downfield region can be recognized simply from their intensity. The spectra were processed with a Gaussian window function to enhance the resolution of the signals in the region 0.5 to  $-2$  ppm.

the use of ultrafiltration using a 30 kDa molecular-weight-cutoff membrane. However, despite the large molecular weight, this protein shows quite sharp

isotropically shifted  $^1\text{H}$  NMR signals. The sharpness of the signals allows us to use 2D NMR techniques for thorough signal analysis. Fig. 2 shows the COSY

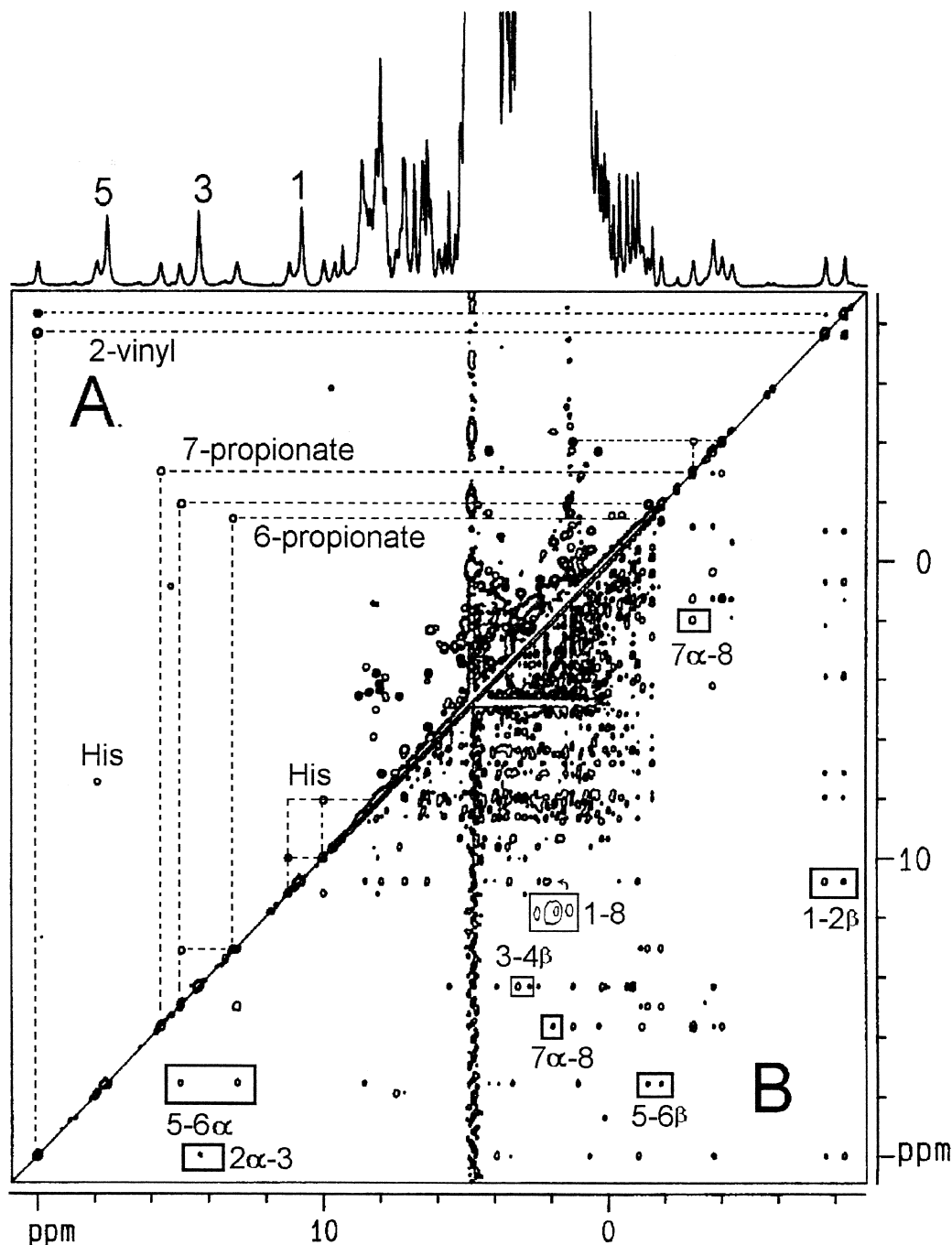


Fig. 2. Proton (A) COSY and (B) NOESY (with a mixing time 100 ms) spectra (360.13 MHz) of the truncated heme-domain from nitrate reductase in  $\text{D}_2\text{O}$  at 298 K. The recycle time is 500 ms in both spectra. The heme vinyl and propionate spin systems are clearly revealed in the COSY spectrum. Some key cross peaks that allow specific heme assignment in the NOESY spectrum are labeled. The inset in the NOESY spectrum shows the “fingerprint” of the methyls 1–8 interaction (the cross peak on the right).

and NOESY spectra of the major species of the NR-heme domain. From the COSY spectrum, the most downfield shifted signal at 20.2 ppm can be easily assigned to a vinyl- $C_{\alpha}$ H proton that has strong through-bond correlation with the vinyl- $C_{\beta}$ H<sub>2</sub> signals at  $-7.6$  and  $-8.3$  ppm. The more intense cross peak between the signals at 20.2 and  $-8.3$  ppm indicates that they are due to the two protons *trans* to each other, which have a larger coupling constant than that of a *cis* pair as observed in all alkene derivatives. The protons of the second vinyl group are located in the diamagnetic region at 5.2 and 3.2/2.8 ppm which can be revealed through 1D NOE experiments and a  $^1\text{H}\{^{13}\text{C}\}$ -HMQC experiment discussed later. The  $C_{\alpha}$ H and  $C_{\beta}$ H<sub>2</sub> protons of the two coordinated His residues are detected, respectively, at 7.18 and 18.0/7.46 ppm, and 8.09 and 11.25/10.01 ppm.

The two propionate groups of the heme can be clearly recognized in the COSY spectrum (Fig. 2(A)). One propionate exhibits proton resonances at 14.9 ( $T_1 = 89.1$  ms), 13.2 (82.2 ms),  $-1.4$  (106.0 ms), and  $-1.9$  (98.2 ms) ppm. The first pair with larger isotropic shifts and shorter  $T_1$  values can be assigned to the geminal  $C_{\alpha}$ H<sub>2</sub> protons and the latter two to the  $C_{\beta}$ H<sub>2</sub> protons. The intense COSY cross peaks between the vicinal pair at 14.9 and  $-1.9$  ppm, and the other pair at 13.2 and  $-1.4$  ppm suggest that these pairs have a *trans* conformation, which affords larger coupling constants thereby more intense cross peaks. Thus, this propionate has a conformation with the carboxylate group and the heme *trans* to each other with respect to the  $C_{\alpha}$ - $C_{\beta}$  bond (Fig. 3). The crystal structure of cytochrome *b*<sub>5</sub> reveals that the heme is bound near the surface of the protein with 7-propionate H-bonded to the consensus Ser 64, and 6-propionate extended out from the protein and stretched into the solvent [34–36]. This stretched *trans* conformation does not allow the carboxylate to be H-bonded with the protein backbone. Thus, the propionate described here with a conformation in which the carboxylate and the heme are *trans* to each other is assigned as propionate-6. This propionate is presumably the only possible moiety on the heme that can interact with the FAD in the flavoprotein domain to foster electron transfer from FAD to the heme on the basis of the crystal structure docking of the cytochrome domain with the FAD domain in corn NR [36].

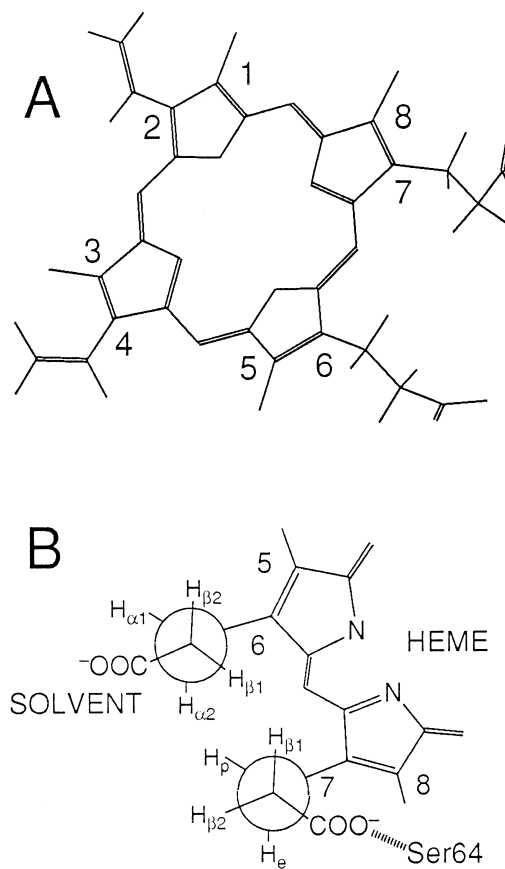


Fig. 3. (A) The schematic structure of protoporphyrin IX, and (B) the conformation of the two heme-propionate viewed from the top of the heme. The propionate-6 has a *trans* conformation and stretches further into the solvent, where the two *trans* vicinal pairs show intense COSY cross peaks; whereas the propionate-7 has a *cis* conformation and bends toward the protein and is H-bonded with a Ser residue based on the crystal structure of bovine cytochrome *b*<sub>5</sub> [34].

The second propionate exhibits proton signals at 15.7 (107.9 ms),  $-3.0$  (128.8 ms), 1.3, and  $-3.7$  ppm (84.1 ms), with the first two and the latter two as the geminal pairs based on the intensities of the cross peaks in the COSY and NOESY spectra (Fig. 2). One interesting feature of this propionate group is that one geminal CH<sub>2</sub> proton pair show dramatically different isotropic shifts and longitudinal relaxation times, reflecting their very different magnetic and/or structural environments; such as with one proton (likely the 15.7 ppm proton) at a more “perpendicular” position with respect to the heme which experiences a better hyperconjugation with the heme  $p_{\pi}$  orbitals

than the one at a more “in-plane” position. The vicinal pair at  $-3.0$  and  $-3.7$  ppm exhibit intense cross peaks in the COSY spectra which reflects their being *trans* to each other with respect to the  $C_\alpha$ – $C_\beta$  bond. The lack of an intense cross peak for the other vicinal pair is indicative of a *cis* conformation for this pair. On the basis of these interactions, the structure of this propionate is revealed to have a “bent” configuration with the carboxylate group *cis* to the heme and *trans* to the 15.7 ppm proton. This configuration allows this propionate to be H-bonded with the protein backbone (Fig. 3). This configuration is similar to that of propionate-7 in bovine cytochrome  $b_5$ , which is H-bonded with a serine side chain (Ser 64) in the crystal structure [34–36]. Despite only  $\sim 30\%$  sequence homology between NR-heme domain and bovine cytochrome  $b_5$  [8], the chemical shift patterns are very similar between these two proteins, particularly the methyl signals (Table 1), suggesting a similar heme binding environment in this protein family.

The  $^1\text{H}$  NMR signals due to the heme can be clearly identified and assigned from a proton–carbon correlation in the  $^1\text{H}\{^{13}\text{C}\}$ -HMQC spectrum (Fig. 4). All the methyl signals from the heme moiety are clearly recognized with  $^1\text{H}$  resonances at 17.7, 14.3, 10.8, and the buried one at 2.0 ppm, and their corresponding  $^{13}\text{C}$  signals at  $-31.3$ ,  $-39.3$ ,  $-18.1$ , and  $-5.7$  ppm, respectively. All six pairs of geminal protons of the vinyl and propionate groups can be clearly observed and assigned in the  $^1\text{H} - \{^{13}\text{C}\}$  correlated 2D map, where one carbon is correlated with two protons (dashed lines in Fig. 4). The  $^{13}\text{C}$  NMR signal of one vinyl- $C_\beta$  is found at 217.0 ppm and its vinyl- $C_\alpha$  is located at 20.1 ppm; and the other vinyl- $C_\beta$  is at 122.5 ppm. One propionate exhibits its  $C_\alpha$  signal at  $-46.0$  ppm and  $C_\beta$  at 145.3 ppm; and the other propionate shows  $C_\alpha$  signal at  $-23.7$  ppm and  $C_\beta$  at 52.6 ppm. In addition, the  $C_\beta$  of a coordinated His is detected at 18.8 ppm.

The NOESY spectra are used to reveal the signals that are attributable to protons close to each other. Three out of the four heme methyl protons can be clearly recognized in the  $> 10$  ppm region based on their signal intensities. The NOESY spectrum in Fig. 2 reveals all the through-space interactions necessary for a complete assignment of the heme moiety. Several NOESY spectra with different mixing times

Table 1

Chemical shift and assignments of proton and carbon-13 NMR of the heme in the truncated heme domain of nitrate reductase at pH 7 (unbuffered) and 298 K.

| Assignment             | Chemical shift for proton (ppm) | Chemical shift for carbon-13 (ppm) | $^1\text{H}$ $T_1$ value (ms) |
|------------------------|---------------------------------|------------------------------------|-------------------------------|
| methyl-1               | 10.8 <sup>a</sup>               | $-18.1^b$                          | 85.5                          |
| vinyl-2 $\alpha$       | 20.2                            | 20.1                               | 53.5                          |
| vinyl-2 $\beta$ t      | $-8.3$                          | 217.0                              | 121.2                         |
| vinyl-2 $\beta$ c      | $-7.6$                          | 217.0                              | 109.4                         |
| methyl-3               | 14.3 <sup>a</sup>               | $-39.3^b$                          | 99.6                          |
| vinyl-4 $\alpha$       | 5.2                             | c                                  | d                             |
| vinyl-4 $\beta$ t      | 3.2                             | 122.5                              | d                             |
| vinyl-4 $\beta$ c      | 2.8                             | 122.5                              | d                             |
| methyl-5               | 17.7 <sup>a</sup>               | $-31.3^b$                          | 74.7                          |
| propionate-6 $\alpha$  | 14.9                            | $-46.0$                            | 89.1                          |
| propionate-6 $\alpha'$ | 13.2                            | $-46.0$                            | 82.2                          |
| propionate-6 $\beta$   | $-1.4$                          | 145.3                              | 106.0                         |
| propionate-6 $\beta'$  | $-1.9$                          | 145.3                              | 98.2                          |
| propionate-7 $\alpha$  | 15.7                            | $-23.7$                            | 107.9                         |
| propionate-7 $\alpha'$ | $-3.0$                          | $-23.7$                            | 128.8                         |
| propionate-7 $\beta$   | $-3.7$                          | 102.4                              | 84.1                          |
| propionate-7 $\beta'$  | 1.3                             | 102.4                              | d                             |
| methyl-8               | 2.0 <sup>a</sup>                | $-5.7^b$                           | d                             |

<sup>a</sup> The corresponding values for methyl-1, 3, 5, and 8 protons in a truncated bovine liver cytochrome  $b_5$  are 11.5, 14.4, 21.8, and 2.7 ppm, respectively (0.1 M phosphate at pH 8.3 and 298 K) [29]; and are 10.6, 14.5, 20.4, and 2.6 ppm, respectively, in *Escherichia coli* ferricytochrome  $b_5$  in 0.1 M phosphate buffer at pH 7.1 and 295 K [37].

<sup>b</sup> The corresponding values for methyl-1, 3, 5, and 8 carbons in the truncated bovine liver cytochrome  $b_5$  are  $-16.6$ ,  $-33.3$ ,  $-34.8$ , and  $-4.6$  ppm, respectively [38]; and at  $-19.3$ ,  $-40.2$ ,  $-37.2$ , and  $-9.1$  ppm, respectively, in the above *Escherichia coli* ferricytochrome  $b_5$  [37].

<sup>c</sup> The corresponding carbon-13 signal is obscured by the residual water signal.

<sup>d</sup> Cannot be measured as signals are buried in the diamagnetic envelope.

(ranging from 50 to 150 ms) were compared, and found to provide virtually the same information for qualitative signal assignment. The methyl at 17.7 ppm shows strong cross peaks with all the four protons of a propionate group, reflecting that this propionate may have a relatively free rotation which affords a chance for all the propionate protons to have a through-space interaction with the methyl group. This suggests that these signals can be assigned to the 6-propionate which is exposed to the solvent and has a higher degree of freedom based on the crystal

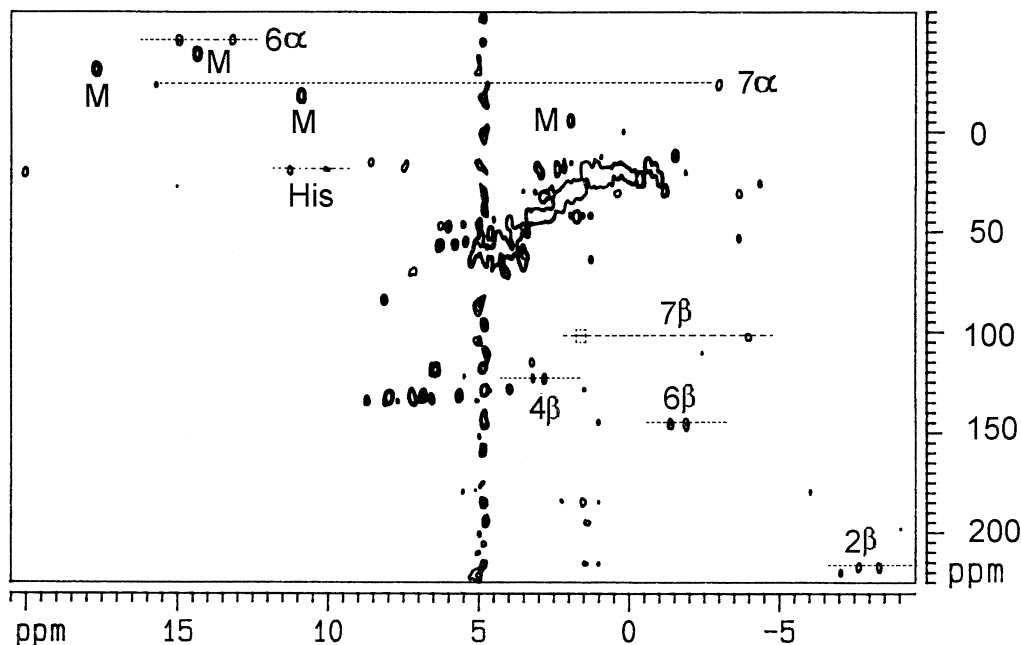


Fig. 4.  $^1\text{H}\{^{13}\text{C}\}$ -HMQC of the truncated NR-heme domain in  $\text{D}_2\text{O}$  at 298 K. The four heme methyl group can be clearly recognized in the upfield region of the  $^{13}\text{C}$  dimension (labeled with M's). Seven  $\text{CH}_2$  signals attributable to the two vinyl, two propionate, and one His- $\text{C}_\beta\text{H}_2$  groups can also be clearly recognized, where one  $^{13}\text{C}$  signal is correlated with two  $^1\text{H}$  signals as shown with dashed lines in the spectrum. The dashed box represents a signal which can be seen only with a lower contour level.

structure of cytochrome  $b_5$  [34–36]. Another pair of propionate  $\text{C}_\alpha\text{H}_2$  at 15.7 and  $-3.0$  (but not  $\text{C}_\beta\text{H}_2$ ) shows cross peaks with the methyl at 2.0 ppm, reflecting a more “rigid” configuration. The NOESY connectivities are also consistent with the propionate configuration revealed in the COSY study, with the *trans* vicinal pairs exhibiting intense COSY cross peaks but only weak NOESY interactions (Fig. 2).

The vinyl- $\text{C}_\alpha\text{H}$  at 20.2 ppm shows weak interaction with the methyl at 14.3 ppm, while its two  $\text{C}_\beta\text{H}_2$  protons have strong cross relaxations with the methyl at 10.8 ppm. The fact that neither of these methyls interact with the propionate groups, but both are close to a common vinyl group, indicates that these methyls are at the 1 and 3 positions. From the NOESY and the  $^1\text{H}\{^{13}\text{C}\}$ -HMQC spectra, another vinyl- $\text{C}_\beta\text{H}_2$  proton pair at 2.8 and 3.2 ppm are also revealed which interact with the methyl signal at 14.3 ppm. At this stage, all the methyl signals can be determined by their correlations with both adjacent vinyl and nearby propionate groups. The “fingerprint” interaction between methyls 1 and 8 is revealed between the signals at 10.8 and 2.0 ppm by both 1D NOE (to

reveal  $1 \leftrightarrow 8$  and  $7 \leftrightarrow 8$  interactions with signals 1 and 7 irradiated, respectively) and NOESY (inset in spectrum B, Fig. 2), which concludes the assignment for all the methyl groups with the signals at 17.7, 14.3, 10.8, and 2.0 ppm assigned to 5-, 3-, 1-, and 8-methyl groups, respectively. Their corresponding propionate and vinyl groups can thus also be assigned accordingly (Table 1).

#### 4. Concluding remarks

The expression of a water-soluble truncated heme domain of *Chlorella vulgaris* NR has allowed a detailed 2D NMR study of the heme moiety. The  $^1\text{H}$  NMR signals of the heme moiety in this NR heme domain have been fully assigned by the use of COSY, NOESY, and  $^1\text{H}\{^{13}\text{C}\}$ -HMQC techniques. The heme structure is similar to that of the membrane-bound bovine cytochrome  $b_5$ ; with 6-propionate exposing to the solvent and having a flexible configuration, and 7-propionate being more rigid and presumably H-bonded to the protein backbone. With the success of

the over-expression and the primary NMR study of this protein, several interesting properties of this enzyme can be pursued in the future; such as the identification of the amino acid residues in the proximity of the heme and structure of the whole heme pocket, the influence of the different heme orientations (Fig. 1) and the heme-pocket structures (via site-directed mutagenesis) on the redox potential and electron transfer rate, the effect of the flavin domain on the electrochemical properties, and the interaction of the protein with its redox partners.

### Acknowledgements

L.-J.M. is grateful for the funds provided by the University of South Florida (USF). A.C.C and L.P.S. acknowledge the support from NSF (Grant MCB 93-17557). X.W. acknowledges a summer fellowship (1995) provided by the Institute for Biomolecular Science at USF. The Bruker AMX360 was purchased with the funds from USF and NSF.

### References

- [1] N.S. Dunn-Coleman, J. Smarelli Jr., R.H. Garrett, *Int. Rev. Cytol.* 92 (1984) 1–50.
- [2] A.B. Thomsett, *Microbiol. Rev.* 2 (1989) 31–55.
- [3] J.L. Wray, J.R. Kinghorn (Eds.), *Molecular and Genetic Aspects of Nitrate Assimilation*, Oxford Science Publications, Oxford.
- [4] L.P. Solomonson, M.J. Barber, *Annu. Rev. Plant Physiol.* 41 (1990) 225–253.
- [5] A.C. Cannons, M.J. Barber, L.P. Solomonson, *J. Biol. Chem.* 268 (1993) 3268–3271.
- [6] A.C. Cannons, N. Iida, L.P. Solomonson, *Biochem. J.* 278 (1991) 203–209.
- [7] G.E. Hyde, N.M. Crawford, W.H. Campbell, *J. Biol. Chem.* 266 (35) (1991) 23542–23547.
- [8] F. Lederer, *Biochimie* 76 (1994) 674–692.
- [9] C. Meyer, J.M. Levin, J.-M. Roussel, P. Rouze, *J. Biol. Chem.* 266 (30) (1991) 20561–20566.
- [10] F.S. Mathews, M. Levine, P. Argos, *Cold Spring Harbor Symp. Quant. Biol.*, vol. 36, 1971, pp. 387–395.
- [11] F.S. Mathews, E.W. Czerwinski, *The Enzymes of Biological Membranes*, Plenum Press, New York, vol. 4, 1976, p. 143.
- [12] C.J. Kay, M.J. Barber, *J. Biol. Chem.* 261 (1986) 14125–14129.
- [13] C.J. Kay, M.J. Barber, L.P. Solomonson, *Biochemistry* 27 (1988) 6142–6149.
- [14] L.P. Solomonson, M.J. Barber, A.P. Robbins, A. Oaks, *J. Biol. Chem.* 261 (1986) 11290–11294.
- [15] L.P. Solomonson, M.J. McCreery, C.J. Kay, M.J. Barber, *J. Biol. Chem.* 262 (1987) 8934–8939.
- [16] C.J. Kay, M.J. Barber, L.P. Solomonson, D. Kau, A.C. Cannons, C.R. Hipkin, *Biochem. J.* 272 (1990) 545–548.
- [17] C.J. Kay, L.P. Solomonson, M.J. Barber, *J. Biol. Chem.* 261 (1986) 5799–5802.
- [18] I. Bertini, C. Luchinat, *NMR of Paramagnetic molecules in biological systems*, Benjamin Cummings, Menlo Park, CA, 1986.
- [19] I. Berliner, J. Reuben (Eds.), *NMR of Paramagnetic Molecule*, *Biol. Magn. Reson.*, vol. 12, Plenum Press, New York, 1993.
- [20] G.N. La Mar (Ed.), *Nuclear Magnetic Resonance of Paramagnetic Macromolecules*, Kluwer, Dordrecht, 1995.
- [21] L.-J. Ming, J.B. Lynch, K.C. Holz, L.J. Que, *Inorg. Chem.* 33 (1994) 83–87.
- [22] L.-J. Ming, X. Wei, *Inorg. Chem.* 21 (1994) 4617–4618.
- [23] L.-J. Ming, *Magn. Reson. Chem.* 31 (1993) S104–S109.
- [24] K. Naqayama, A. Kumar, K. Wüthrich, R.R. Ernst, *J. Magn. Reson.* 40 (1980) 321.
- [25] J.H. Noggle, R.E. Schirmer, *The Nuclear Overhauser Effect*, Academic Press, New York, 1971.
- [26] D. Neuhaus, M.P. Williamson, *The Nuclear Overhauser Effect in Structural and Conformational Analysis*, VCH, New York, 1989.
- [27] A. Bax, D.G. Davis, *J. Magn. Reson.* 65 (1985) 355–360.
- [28] A. Bax, S. Subramanian, *J. Magn. Reson.* 67 (1986) 565–569.
- [29] S.J. Mclachlan, G.N. La Mar, P.D. Burns, K.M. Smith, K.C. Langry, *Biochim. Biophys. Acta* 874 (1986) 274–284.
- [30] K.-B. Lee, G.N. La Mar, L.A. Kehres, E.M. Fujinari, K.M. Smith, T.C. Pochapsky, S.G. Sligar, *Biochemistry* 29 (1990) 9623–9631.
- [31] T.C. Pochapsky, S.G. Sligar, S.J. Mclachlan, G.N. La Mar, *J. Am. Chem. Soc.* 112 (1990) 5258–5263.
- [32] K.-B. Lee, G.N. La Mar, R.K. Pandey, I.N. Rezzano, K.E. Mansfield, K.M. Smith, T.C. Pochapsky, S.G. Sligar, *Biochemistry* 30 (1991) 1878–1887.
- [33] S.L. Alam, D.P. Dutton, J.D. Satterlee, *Biochemistry* 33 (1994) 10337–10344.
- [34] F.S. Mathews, P. Argos, M. Levine, *Cold Spring Harbor Symp. Quant. Biol.*, vol. 36, 1972, p. 387.
- [35] G. Lu, Y. Lindqvist, G. Schneider, U. Dwivedi, W. Campbell, *J. Mol. Biol.* 248 (1995) 931–948.
- [36] Z.-X. Xia, F.S. Mathews, *J. Mol. Biol.* 212 (1990) 837–863.
- [37] L. Banci, I. Bertini, R. Pierattelli, A.J. Vila, *Inorg. Chem.* 33 (1994) 4338–4343.
- [38] K.-B. Lee, J. Kweon, H. Park, *FEBS Lett.* 367 (1995) 77–80.